Handbook of Geospatial Approaches to Sustainable Cities

Edited by Qihao Weng in collaboration with Cheolhee Yoo

First published 2024

ISBN: 978-1-032-15481-7 (hbk)
ISBN: 978-1-032-15534-0 (pbk)
ISBN: 978-1-003-24456-1 (ebk)

7

The Potential of Nature-Based Solutions in Urban Heat Mitigation and Building Energy Savings

Siqi Jia, Qihao Weng, and Yuhong Wang

DOI: 10.1201/9781003244561-9

The Open Access version of this chapter was funded by Qihao Weng.

CRC Press
Taylor & Francis Group
Boca Raton London New York

CRC Press is an imprint of the
Taylor & Francis Group, an **informa** business

7 The Potential of Nature-Based Solutions in Urban Heat Mitigation and Building Energy Savings

Siqi Jia, Qihao Weng, and Yuhong Wang

INTRODUCTION

Given the frequency and severity of heatwaves and Urban heat islands (UHI), there has been a growing awareness of the UHI and urban thermal environment (Ketterer & Matzarakis, 2015; Kim & Brown, 2021; Su et al., 2022). The increasing urban heat not only traps atmospheric pollutants, deteriorates the conditions of living environments, and increases energy consumption (Herath et al., 2018), but it also affects health, leisure activities, and well-being of urban dwellers (Doick et al., 2014; Feyisa et al., 2014; Halder et al., 2021). With more than half the world's population currently residing in cities and this number expected to rise to around 70% by 2050 (Profiroiu et al., 2020; Ritchie & Roser, 2018), combatting the adverse effects of urban heat has become a pressing global issue for both the environment and human beings. Consequently, it is crucial to develop effective heat mitigation solutions to alleviate these challenges (Aram et al., 2019; Wong et al., 2021).

Nature-based solutions (NBS) are increasingly recognized as effective measures to address the challenges of UHI and heatwaves by providing cooling services (Lafortezza et al., 2018; Su et al., 2022), and therefore help to increase energy efficiency. It can foster and simplify implementation actions in urban landscapes by taking into account the service provided by nature (Kabisch et al., 2017). Moreover, it is highlighted that NBS can be cost-effective and that benefits range from environmental protection to creating jobs that stimulate innovation for a green economy. Examples of NBS include provision of urban greenspace such as parks, street trees, and green infrastructure (e.g., green roof, green façade) that may ameliorate high temperature in cities or regulate air and water flows (Gill et al., 2007; Yamamoto, 2006). In this research, the performance of three commonly used NBS in urban heat mitigation and building

DOI: 10.1201/9781003244561-9

energy savings are introduced, including green roof, evaporative pavement, and street trees. Numerous studies have shown that NBS are effective in heat mitigation and energy use reduction (A. Niachou, 2001; Castleton et al., 2010; Romeo & Zinzi, 2013; Zheng & Weng, 2020), while their efficiency is significantly influenced by local climate conditions and building characteristics. However, most of those studies have only considered a few selected buildings in case studies or have focused primarily on the summer season (Costanzo et al., 2016; He et al., 2020), leading to a lack of research on how variations in ambient climate and built environment influence the energy-saving potential of these technologies.

Building energy consumption is greatly susceptible to meteorological feedback, which refers to the dynamic interactions between the building and the surrounding environment, particularly local weather conditions (Li et al., 2019). The heating, cooling, and ventilation requirements of a building are influenced by meteorological feedback, which can have a significant impact on energy consumption (Wong et al., 2011; Yu & Hien, 2006). Accurate prediction and modeling of meteorological feedback is crucial for optimizing building energy performance and reducing energy consumption. However, most existing building energy simulation models used Typical Meteorological Year (TMY) weather files to represent historical and current weather conditions (Fumo, 2014; Hosseini et al., 2020), while failed to incorporate ambient micro-scale climatic conditions and ensure accurate results in energy simulations.

Overall, a comprehensive study that compares these typical NBS in different climate settings is called for. To improve the model accuracy, this study proposes a new integrated approach to study the potential of building energy reductions by different NBS. This approach combines climate change modeling and building energy simulation to quantify the effect of climate change on building energy demand. The research objectives include: 1) to evaluate the effectiveness of NBS in urban heat mitigation; 2) to evaluate the effectiveness of NBS in building energy savings; 3) to identify the influencing factors affecting the performance of typical NBS in different urban built environments and climates. The results of this study can help policymakers and urban planners make informed decisions about the implementation of NBS in their respective cities, leading to greater sustainability and resilience of urban areas in the face of climate change. Furthermore, the study contributes to advancing the scientific understanding of the role of NBS in urban planning and highlights the importance of developing solutions that are tailored to specific local conditions.

NATURE-BASED SOLUTIONS FOR URBAN HEAT MITIGATION AND BUILDING ENERGY SAVINGS

In this research, the performance of three commonly used NBS in urban environment was evaluated, including green roof, evaporative pavement, and street trees. This section covers the mechanism, effectiveness, advantages, and limitations of each NBS.

Green Roofs

A green roof is a layered system that includes a waterproofing membrane, growing medium, and vegetation layer (Castleton et al., 2010). It has become an increasingly popular design strategy for improving urban environments due to its numerous environmental benefits, including reducing stormwater flow, improving air quality, and mitigating the Urban Heat Island (UHI) effect (Barrio, 1998; Berardi, 2016). Green roofs are widely recognized to mitigate increased urban temperatures, particularly in hot climates, where they can reduce temperatures to more comfortable levels (Razzaghmanesh et al., 2016). During winter conditions, they offer effective thermal protection by providing high insulation levels that strangle heat flux (He et al., 2017; Theodosiou, 2003). Green roofs can also lower cooling energy costs by 32% to 100% (Susca et al., 2011), while reducing heating energy demands by 23% (Zhao et al., 2015).

Green roofs can be classified into two types based on their purpose and characteristics: extensive green roofs (EGR) and intensive green roofs (IGR) (Townshend, 2007). EGR is covered with grass only and is designed to be self-sustaining. In contrast, IGR is usually associated with rooftop gardens and requires skilled labor, irrigation, and constant maintenance due to the deeper soil depth needed for growing trees and other vegetation (Bianchini & Hewage, 2012). IGR typically has thicker growing media and higher canopy density, resulting in higher levels of evapotranspiration and shading than EGR. This results in lower outdoor surface temperatures and better cooling effects (Castleton et al., 2010; Silva et al., 2016). However, IGR requires higher capital costs and technical expertise for installation and maintenance compared to EGR, which offers more economic benefits (Townshend, 2007). Figure 7.1 shows the appearance of both types of green roofs.

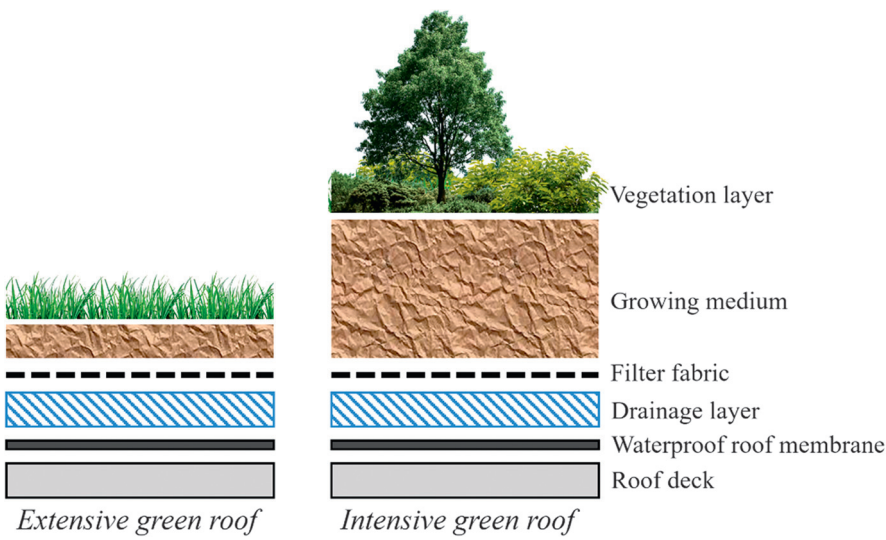

FIGURE 7.1 Extensive green roof and intensive green roof.

Nevertheless, although urban heat mitigation through roof-level strategies has often been investigated, the effectiveness of heat mitigation strategies in improving the pedestrian-level thermal environment has been questioned. For instance, because of the height of roofs, some researchers believed that the pedestrian-level cooling effects of green roofs are negligible (Chen et al., 2009; Zölch et al., 2016). In contrast, the street-level heat mitigation strategies are believed to be more effective in improving pedestrian's thermal comfort through shading, evaporation, and evapotranspiration (Morakinyo, Dahanayake, et al., 2017; Taleghani, 2018).

Evaporative and Water-Retentive Pavements

Evaporative and water-retentive pavements allow water to pass through their material voids, thereby facilitating its penetration into the soil. These pavements rely on evaporation of the water for the maintenance of a desirable thermal environment. Higher moisture contents and increased watering can help keep the pavement surface cooler. To achieve their water-retentive and permeable properties, these pavements eliminate finer particles from their structure or replace them with more porous materials such as pozzolans, slag, fly ash, or silica fumes (Mohajerani et al., 2017). The porosity of these materials imparts a lower albedo compared to impermeable counterparts, and enhances convective fluxes to the atmosphere by increasing the effective surface area via higher void content (Haselbach, 2009; Santamouris, 2013). According to ITO (ITO, 2006), water-retentive pavements can reduce surface temperatures by up to 16°C and air temperatures by approximately 1°C, contributing to the UHI mitigation. Another study on surface heat budgets demonstrated that adding water-retaining materials to asphalt and cement concrete surfaces significantly reduced sensible heat flux at rates of 150 W/m^2 and 100 W/m^2, respectively (Takebayashi & Moriyama, 2012). The effectiveness of evaporative and water-retentive pavements may be limited by climatic conditions (Santamouris, 2013). They are more suited to warm and humid climates where rainwater is a significant factor in cooling pavement surfaces. Figure 7.2 shows the progress of how water-retentive pavements cool the environment.

Street Trees

Urban areas can benefit from large tree or shrub-type greenspaces as they provide notable cooling through shade, evapotranspiration, and increased albedo (Wong et al., 2021). The cooling effect and thermal comfort improvement of trees depend on factors such as leaf area index, tree height, trunk height, and spatial configuration of trees (Morakinyo, Kong, et al., 2017; Tan et al., 2016; Zhou et al., 2017). Numerous studies have highlighted the effectiveness of implementing trees for outdoor heat mitigation in high-density urban settings (Morakinyo, Kong, et al., 2017; Thom et al., 2016). For example, Cheung and Jim (2018) compared the cooling effects of a tree and a concrete shelter, identifying that the tree provides significantly better cooling effects than the shelter with the mean daytime air temperature reduction at 0.6 °C and the maximum daytime air temperature

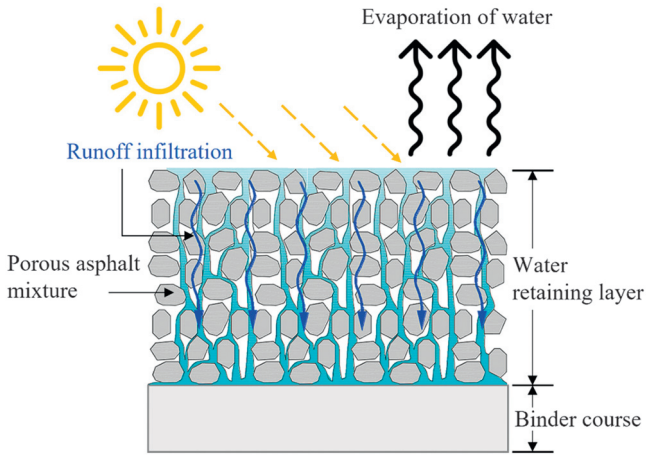

FIGURE 7.2 Water-retentive pavement.

reduction at 2.1 °C (Cheung & Jim, 2018a). Another study used high-resolution satellite data of 293 European cities to investigate the effectiveness of urban trees in mitigating urban heat. Results showed that the surface temperature observed for urban trees is on average 0–4 K lower in Southern European regions and 8–12 K lower in Central Europe (Schwaab et al., 2021). Increasing tree canopy in open and exposed streets should be given priority to achieve the greatest improvement in outdoor thermal comfort (Thom et al., 2016). However, the cooling effect of small greenspace with few trees or shrubs and grass-type greenspace has been questioned. Some studies have suggested that these types of greenspaces are more susceptible to urban and anthropogenic influences, which may increase sensible heat gain instead of providing cooling (Wong et al., 2021). Figure 7.3 shows an example of the typical design of street trees.

FIGURE 7.3 Street trees. Source: Google Map, captured at Nathan Road, Kowloon, Hong Kong.

METHODOLOGY

Assessment of Thermal Comfort

Mean Radiant Temperature

To objectively assess the thermal comfort level of a space, four crucial meteorological variables that govern the human energy balance and outdoor thermal comfort are typically utilized. These include air temperature (T_a), relative humidity (rH), wind speed (V_a) and mean radiant temperature (T_{mrt}). Particularly, T_{mrt} is a critical metric for human thermal comfort assessment (Mayer & Höppe, 1987; Thorsson, Lindberg, et al., 2007) for it is a quantity linking the radiant energy transfer between a human body and surroundings to which the body exposed (ASHRAE, 2013). While all other meteorological parameters can be obtained from on-site sensors, there are two common methods for directly measuring T_{mrt}: the integral radiation method and the globe thermometer method (Thorsson, Honjo, et al., 2007).

The integral radiation method, which was proposed by Höppe in 1992 (Höppe, 1992), has been widely recognized as the most accurate T_{mrt} measurement method (Thorsson, Lindberg, et al., 2007; VDI, 1998; Walikewitz et al., 2015). It is an experimental method that involves the measurement of short-wave and long-wave radiant flux densities emitted from the entire three-dimensional environment (Höppe, 1992; Manavvi & Rajasekar, 2020). However, it is difficult to undertake multi-point observations by this method in outdoor experiments with respect to the high cost and complexity of measurement setup. Therefore, the observations using the integral radiation method are often used as a reference to compare or modify the results of other methods (Chen et al., 2014; Crank et al., 2020; de Lieto Vollaro et al., 2013). Another commonly used method to obtain an estimate of T_{mrt} directly is the globe thermometer method. The black-globe thermometer method has been in use since it was first developed in the 1930s and then quickly gained attention due to its simplicity (Bedford & Warner, 1934). Referring to Kuehn et al. (Kuehn et al., 1970), assuming the globe thermometer is in equilibrium, the globe temperature, which is expressed as the weighted average of radiant and ambient temperatures, reflects the convective and radiative heat exchange around the black-globe thermometer. The globe thermometer method was initially developed to measure indoor radiant temperature. For outdoor use, an empirical equation is required to predict T_{mrt} based on additional parameters including the wind speed and air temperature (Eq. 7.1):

$$T_{mrt} = \left[(T_g + 273.15)^4 + \frac{1.1 \times 10^8 V_a{}^{0.6}}{\varepsilon D^{0.4}} \times (T_g - T_a) \right]^{1/4} - 273.15 \qquad (7.1)$$

where T_g is the globe temperature ($^\circ C$), V_a is the air velocity (m/s), T_a is the air temperature ($^\circ C$), D is the globe diameter (mm), and ε is the globe emissivity. However, the globe thermometer method has some shortcomings in outdoor applications. For example, previous studies revealed the unsuitability of the globe thermometer for T_{mrt} measurement in an outdoor situation, given the constantly changing radiative fluxes and air velocity may prolong the time to reach equilibrium (Spagnolo & de Dear, 2003).

Outdoor Thermal Comfort Indices

Researchers have dedicated substantial effort towards developing metrics for quantifying human thermal comfort (Herrmann & Matzarakis, 2010; Höppe, 1999; Makaremi et al., 2012). Human thermal comfort is described as a state of mind that reflects satisfaction or dissatisfaction with the surrounding environment (Abdel-Ghany et al., 2013). An individual's thermal state is affected by micro-climatic conditions such as wind speed, temperature, humidity, and the positions of sun and shade (Cheng et al., 2011; Comfort, 2003; Lai et al., 2014). To assess outdoor thermal comfort, several indices integrating environmental factors and the energy balance of the human body have been developed (Xi et al., 2012). Some examples of these indices are the Predicted Mean Vote (PMV), Physiological Equivalent Temperature (PET), and Universal Thermal Climate Index (UTCI) (Fang et al., 2019; Lai et al., 2014; Provencal et al., 2016).

Although all of these indices have been applied to assess human responses to the environment, the use of steady-state indices (e.g., PMV) may lead to estimation errors for pedestrians in an outdoor environment where dynamic thermal adaptation and transient process are involved. For instance, studies by Nikolopoulou et al. (Nikolopoulou et al., 2001) and Lai et al. (Lai et al., 2014) found significant discrepancies between a person's subjective thermal satisfaction and objective thermal states described by PMV. Hence, recent studies commonly use PET and UTCI as outdoor thermal indices (Cheung & Jim, 2018b). Both indices simulate dynamic heat transport within the body and the heat exchange between the body and its environment (Fiala et al., 1999, 2001). Compared to the two-node models used for PET, multi-node models used for UTCI provide more detailed simulations of the human body, predicting both overall (whole-body) and local (multi-node) physiological responses (Fang et al., 2019; Jia & Wang, 2021; Rakha, 2015). Therefore, this study employed UTCI to represent outdoor thermal comfort.

Microclimatic Modeling

ENVI-met

For simulating the meteorological parameters and universal thermal indices, ENVI-met has been applied to account for the thermal exchange of every location in the environment with fine resolutions. ENVI-met is a Computational Fluid Dynamics (CFD) based microclimate and local air quality model. ENVI-met is capable of calculating both surface temperature and air temperature of different heights within the interval times for 24 to 48 hours (Hien et al., 2012). Key input parameters include weather conditions, initial soil wetness and temperature profiles, structures, the physical properties of urban surfaces, and plants (Berardi, 2016). ENVI-met can simulate the long-wave and short-wave radiative exchange within the plants, the plant canopy effects on convective heat transfer, evapotranspiration from soil and plants, heat conduction in the soil layer, and moisture-dependent thermal properties (Sailor, 2008; Yang et al., 2019; Zölch et al., 2016). ENVI-met consists of a one-dimensional (1D) boundary sub-model which is used to calculate the inflow profile and top boundary, a

three-dimensional (3D) atmospheric sub-model which is the main model, and a 3D/1D soil sub-model (Huttner, 2012). Flow simulation in the atmospheric model is based on the Reynold-averaged Navier-Stokes (RANS) equations (Acero & Arrizabalaga, 2016), and Yamada and Mellor E-ε (Yamada & Mellor, 1975) is chosen as the turbulence model. Further details of ENVI-met can be found in the literature (Ali-Toudert & Mayer, 2006; Bruse & Fleer, 1998).

Scenario Development

The computational domain in this study is set as $x \times y \times z = 250$ m $\times$ 250 m $\times$ 200 m. Both the buildings and streets in the study area are carefully modeled. Key input parameters include weather conditions, initial soil wetness and temperature profiles, structures, the physical properties of urban surfaces, and plants (Berardi, 2016). Three types of land cover are considered for the walkways: soil, permeable surface using grasscrete paver, and asphalt pavement. Default albedo values are used for each type of land cover. The buildings (height: 30 m) and trees (height: 5 m, canopy width: 5 m) are distributed on these land cover types. Additional simulation details are shown in Table 7.1.

The base scenario represents the current outdoor microclimate, urban layout, and surface conditions of the study area. Additional simulation scenarios are developed for evaluating the influences of different types of heat mitigation strategies on outdoor microclimate and thermal comfort. The details of each simulation scenario are shown in Table 7.2, and the layouts of scenarios are displayed in Figure 7.4. The influences of four types of heat mitigation strategies (EGR, IGR, ST, and PP) and the reference (REF) on outdoor microclimate and thermal comfort are evaluated based on the outputs of ENVI-met, including surface air temperature (T_a), mean radiant temperature (T_{mrt}), relative humidity (rH), and wind speed (V_a).

TABLE 7.1
ENVI-met Simulation Details

Start and Duration of the Simulation	
Start date	1st August 2020
Start time	0:00 am
Total simulation time period (h)	24
Domain size and grid resolution	
Size of computational domain (dx, dy, dz)	250 m × 250 m × 200 m
Grid resolution (dx, dy, dz)	2 m × 2 m × 2 m
Initial meteorological conditions	
Air temperature range (°C)	22–34
Wind speed at the height of 10 m (m/s)	2.5
Wind direction (deg)	0°
Roughness length at the measurement site (m)	0.1
Relative humidity (%)	60 –70

TABLE 7.2
Description of Simulation Scenarios

Scenarios	Details
Extensive green roof (EGR)	Buildings are installed with extensive green roofs (covered by grass)
Intensive green roof (IGR)	Buildings are installed with intensive green roofs (covered by shrubs and small trees)
Permeable pavement (PP)	The pavement is covered by the permeable surface using grasscrete paver
Street tree (ST)	More street trees are added on vacant spaces along the sidewalks

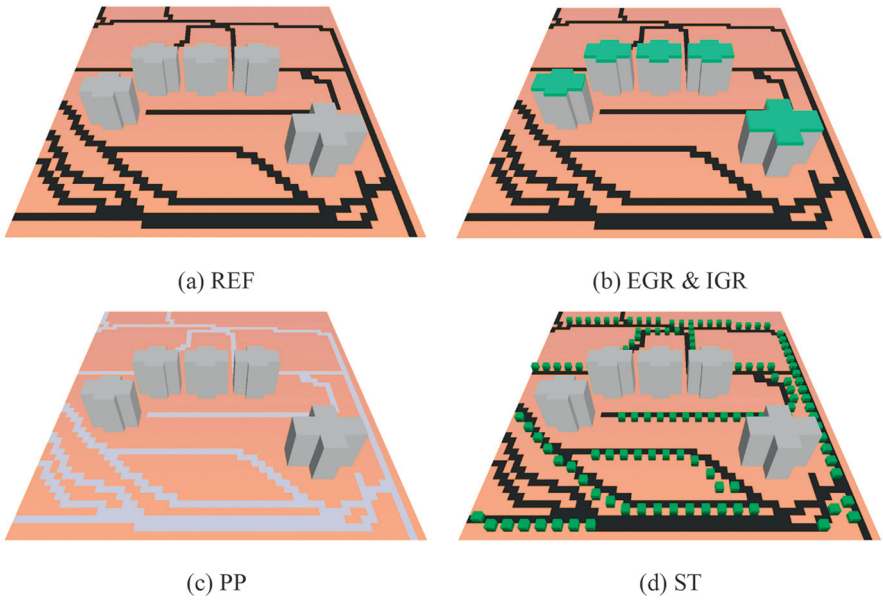

FIGURE 7.4 The layouts of simulation scenarios: (a) reference (REF); (b) extensive green roof (EGR) & intensive green roof (IGR); (c) permeable pavement (PP); and (d) street trees (ST).

Validation of the Meteorological Outputs

The general validity of the ENVI-met model was evaluated from an experimental site in Hong Kong (Figure 7.5(a)). The experimental area is 100 m × 100 m with a grid resolution of 0.5 m. Two sets of experiments were conducted under sunny conditions on different dates and seasons (October 29–31, 2020; April 3–5, 2021) at the same site. The diurnal profiles obtained from the three-day observations were used to validate the model.

To measure and record the background weather parameters, a Kestrel 5400 weather station (Nielsen-Kellerman Co. USA) was set up at a height of 1.5 m above the ground level (Figure 7.5(b)). The following parameters were measured: air temperature (T_a, range: −29 to 70 °C), globe temperature (T_g, range: −29 to 70 °C),

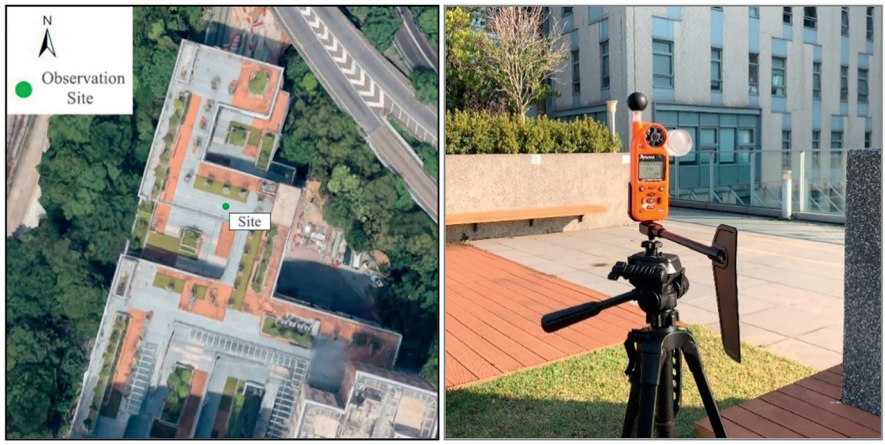

FIGURE 7.5 The experimental site (a) and experimental setup (b).

relative humidity (*rH*, range: 10 to 90%), wind speed (V_a, range: 0 to 40 m/s), and wind direction (range: 0 to 360 °C). The mean radiant temperature (T_{mrt}) based on the globe thermometer method (Chen et al., 2014; Mehrotra et al., 2019; Standard & ISO, 1998; Tan et al., 2013) was calculated using the globe temperature, air temperature, and wind speed data. In the second experiment, another Kestrel weather station was installed at the inlet boundary of the modeled area to measure the inlet wind speed. The global radiation data was collected with a CMP 3 Kipp & Zonen pyranometer to calculate the solar radiation adjustment factor in ENVI-met. The hourly mean values of air temperature and relative humidity during the modeled time period were used for simple forcing in ENVI-met to perform the simulations.

The outputs were compared with the diurnal profiles of measured meteorological variables. Table 7.3 provides two error terms obtained from ENVI-met and field measurements: the mean absolute error (MAE), and the error range. The relatively low MAE values in both experiments indicate that the prediction results for the four meteorological parameters are partially accurate. ENVI-met was then applied to the scenario analysis in this study.

TABLE 7.3
Estimation Errors of Meteorological Parameters in Two Experiments

	Autumn (October 2020)		Spring (April 2021)	
	MAE	**Range**	**MAE**	**Range**
T_a (°C)	0.82	−1.70 ~ 1.12	1.15	−3.79 ~ 0.76
T_{mrt} (°C)	1.01	−4.28 ~ 2.61	1.96	−5.79 ~ 3.87
rH (%)	3.40	−3.91 ~ 10.19	2.84	−2.51 ~ 12.22
V_a (m/s)	0.11	−0.19 ~ 0.21	0.17	−0.41 ~ 0.17

Building Energy Simulation

EnergyPlus

This research proposes an integrated modeling approach that combines ENVI-met and a building energy simulation program (i.e., EnergyPlus). Figure 7.6 illustrates the development of the integrated modeling approach. The model first simulates microclimatic conditions in various urban built environments under different climates using ENVI-met. For the model inputs, the climate conditions incorporate the climates of six evaluated cities, while the built environments incorporate the typical urban building types based on the local climate zone (LCZ) system. Case studies were conducted in six selected cities in different climatic zones around the world, including Cairo, Hong Kong, Seoul, London, Los Angeles, and Sao Paulo. The forcing weather data required for the simulations was obtained from

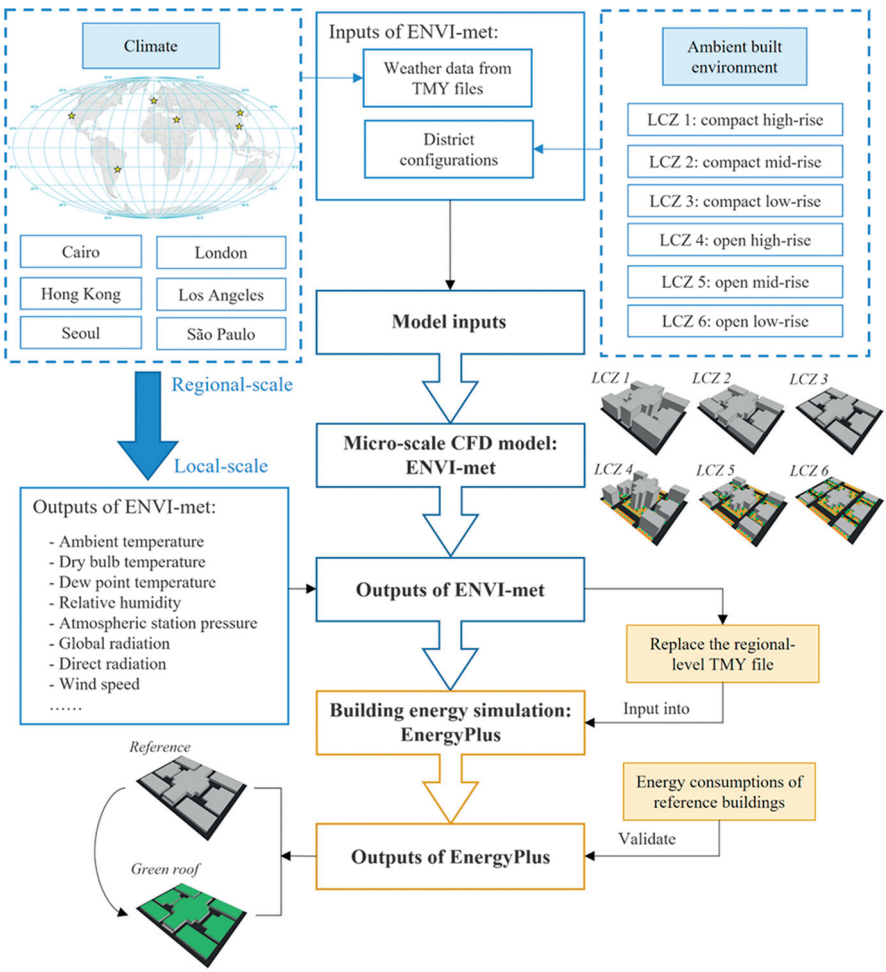

FIGURE 7.6 Development of the integrated modeling approach.

EnergyPlus Weather (EPW) files for each city. ENVI-met can generate much more detailed meteorological outputs (e.g., ambient temperature, relative humidity, wind speed, and reflectance) compared to the region-level EPW files. The outputs of ENVI-met are then used to configure EnergyPlus by modifying the TMY weather inputs. Based on the micro-scale environmental parameters, the detailed building energy use is simulated for different modeled environments. EnergyPlus is an open-source simulation program used for estimating building energy use, including heating, cooling, ventilation, and lighting (Crawley et al., 2001). It enables users to model buildings with mechanical and electrical systems that have integrated thermal controls and perform simulations based on real building descriptions (Morakinyo, Dahanayake, et al., 2017). EnergyPlus has been widely used to help optimize building energy performance and improve indoor thermal comfort while reducing energy consumption (Fumo et al., 2010).

The integrated modeling framework described in this research offers a powerful tool for conducting detailed observations and simulations of local physical environments and meteorological conditions. This approach can lead to more accurate estimations of building energy use compared to traditional modeling methods. In this study, the framework is then applied to a set of scenarios after validation. The scenario development involved modeling the building energy use with or without energy-saving solutions in different ambient climates and urban built environments. By comparing the results of these simulations with those of the baseline scenarios, we are able to determine the effectiveness of cool and green roofs for reducing building energy use in different environments.

Scenario Development

mong the three evaluated NBS (i.e., green roof, permeable pavement, and street trees), only the building energy-saving performance of roof-level strategies (i.e., green roof) was evaluated. For scenarios incorporating the effect of ambient climate, the distinct climate of six typical cities around the world was incorporated into scenarios evaluating the energy-saving performance of green roofs. For scenarios incorporating the effect of urban built environment, six scenarios incorporating different urban built environments were constructed according to the LCZ system (Stewart & Oke, 2012; Zheng et al., 2018). LCZs are being used in the numerous studies focusing on temperature, rainfall, and other environmental variables (Das & Das, 2020; Patel et al., 2023; Yang et al., 2021; Yang et al., 2022). In this study, each scenario corresponds to a different LCZ, including: 1) Scenario a (LCZ 1, compact high-rise environment); 2) Scenario b (LCZ 2, compact mid-rise environment); 3) Scenario c (LCZ 3, compact low-rise environment); 4) Scenario d (LCZ 4, open high-rise environment); 5) Scenario e (LCZ 5, open mid-rise environment); and 6) Scenario f (LCZ 6, open low-rise environment). Table 7.4 presents geometric and surface cover properties for each LCZ.

The layout corresponding to each LCZ was modeled in ENVI-met. The computational domain in this study was set as $X \times Y = 200\ m \times 225\ m$, with grid cells of 5 m. Two types of land cover – natural surfaces (covered by soil) and concrete pavement – were considered to characterize the pervious and

TABLE 7.4
Geometric and Surface Cover Properties for Each LCZ

LCZ	Description	Sky View Factor	Aspect Ratio	Building Surface Fraction (%)	Impervious Surface Fraction (%)	Pervious Surface Fraction (%)	Height (m) of Roughness Elements
LCZ 1	Compact high-rise	0.2–0.4	>2	40–60	40–60	<10	>35
LCZ 2	Compact mid-rise	0.3–0.6	0.75–2	40–70	30–50	<20	10–25
LCZ 3	Compact low-rise	0.2–0.6	0.75–1.5	40–70	20–50	<30	3–10
LCZ 4	Open high-rise	0.5–0.7	0.75–1.-25	20–40	30–40	30–40	>25
LCZ 5	Open mid-rise	0.5–0.8	0.3–0.75	20–40	30–50	20–40	10–25
LCZ 6	Open low-rise	0.6–0.9	0.3–0.75	20–40	20–50	30–60	3–10

Source: Stewart & Oke (Stewart & Oke, 2012).

impervious surfaces within the modeled space, respectively. Default albedo values were used for the different types of land cover. For modeled spaces of compact urban densities corresponding to LCZs 1 to 3, the building surface fraction was 60%, while the impervious surface fraction was 40%. A total of seven buildings were uniformly distributed on the concrete surfaces, and there was no previous surface among these three modeled spaces. For LCZs 4 to 6, six buildings were included in the modeled environment, with a total building surface fraction of 30%. The impervious and pervious surface fractions were 40% and 30%, respectively. Trees (height: 10 m) and shrubs (height: 0.5 m) were uniformly distributed on the natural surfaces with a canopy width of 10 m. Assuming an average floor height of 3 m, the building heights for all buildings within the modeled space ranged from 30 to 60 m (10–20 story height) for LCZs 1 and 4, 15 – 24 m (5–8 story height) for LCZs 2 and 5, and 3 – 9 m (1–3 story height) for LCZs 3 and 6.

Validation of the Building Energy Use

The proposed methodology was validated using a building energy dataset obtained from the U.S. Department of Energy's Building Technologies Office (Luo et al., 2022). The target building is a medium-sized office building (i.e., Building 59), located in Berkeley, California. The building has four floors (only the top two floors are the office floors) and a conditioned space of 10,400 m^2. The building's roof is composed of a white single-ply PVC roofing membrane installed on a concrete roof deck. Figure 7.7 depicts the appearance and layout of the model building.

The dataset comprises hourly data of whole-building and end-use energy consumption, HVAC system operating conditions, outdoor and indoor

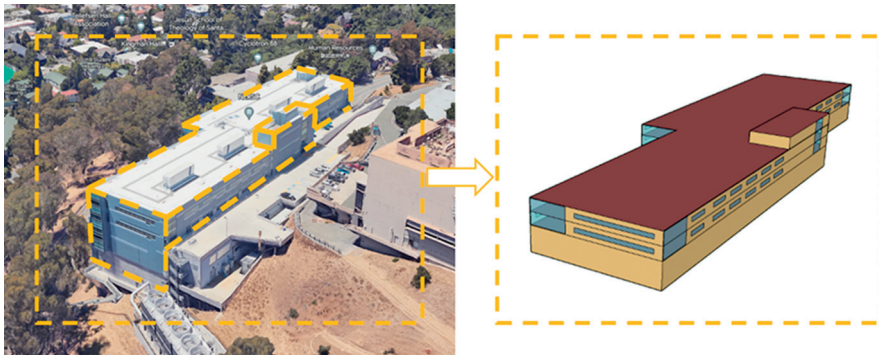

FIGURE 7.7 Appearance and layout of the model building.

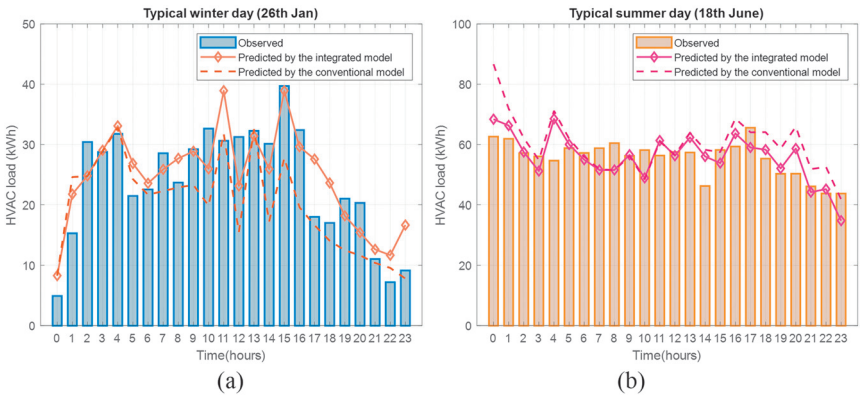

FIGURE 7.8 Accuracy of the hourly energy use simulation: (a) on a typical winter day; (b) on a typical summer day.

environmental parameters, and occupant data. The dataset covers a period of three years from 2018 to 2020. To validate the accuracy of the proposed integrated method, we first simulated the diurnal profiles of energy consumption in the reference office building for a typical winter day and summer day. We then compared the simulated hourly profiles with the observed hourly building energy use on those two days. After validation, the proposed method was used to simulate building consumption in various scenarios. The diurnal profiles of energy consumption in the reference office building were simulated on two typical days: the day with the minimum daily ambient temperature (January 26, and the day with the maximum temperature (June 18). Figure 7.8 shows the accuracy of the simulated hourly building use by the integrated modeling approach on both days, along with the building energy use predicted by the conventional method with inputting the regional weather data as a comparison.

The proposed method using micro-level weather data is capable of accurately simulating building energy use at a high temporal resolution. On a typical winter day (Figure 7.8(a)), the proposed method reduces the root-mean-square error

(RMSE) from 7.25 kWh (1.27%) with the conventional method to 4.96 kWh (0.87%). On a typical summer day (Figure 7.8(b)), the proposed method also outperforms the conventional method with an RMSE of 6.08 kWh (0.46%), which is 3.09 kWh lower than that of the conventional method (0.69%). This method has further potential applications for building energy simulations in various climates and built environments after further validation.

RESULTS

Performance of Nature-Based Solutions in Urban Heat Mitigation

The heat mitigation potentials of the different types of heat mitigation strategies are analyzed. Figure 7.9 presents the diurnal air temperature, mean radiant temperature, and UTCI at the pedestrian-level (at a height of 1.5 m) of the walkways for the five simulation scenarios (one reference and four NBS). Note that the temperature shown in the figure is the average temperature of all the points on the walkways for each simulation scenario.

The figure reveals the effectiveness of different types of heat mitigation strategies at improving the thermal environment, especially between 13:00 and 17:00 when it is the hottest. All evaluated NBS can cause some reductions in air temperature. Compared with the reference, street trees cause a maximum reduction in air temperature and mean radiant temperature by 0.27 °C and 4.23 °C, respectively. According to Figure 7.9(c), street trees also result in the lowest values of UTCI during the daytime, with a maximum UTCI reduction of 0.8817 °C at 11:00. The UTCI values of all other heat mitigation strategies are only slightly lower than those of the reference. At night, there is almost no difference in UTCI values among all of the scenarios, except for the slightly increased values under the ST scenario. Notably, the thermal environment may affect air conditioning use in the neighborhood, as lower environmental temperatures may be associated with less heat emission from air conditioning. This factor, however, is not incorporated into estimates of UTCI values. Next, the distributions of UTCI reductions compared to the reference are shown in Figure 7.10. UTCI reduction value is calculated by subtracting the UTCI value of the simulation scenario from the reference value at the same position. All of the values in the figure are obtained from the simulation results at 16:00 when the reference's UTCI reaches a maximum.

Figure 7.10 reveals that there is an interactive effect between the location and type of heat mitigation strategy. For the roof-level NBS (EGR and IGR, see Figure 7.10(a) and (b)), the effects of green roofs on improving pedestrian-level thermal comfort are more noticeable along the E–W directions of buildings, and the thermal comfort improvement is more obvious in the S-W corner of the study area. In the PP scenario (Figure 7.10(d)), the biggest UTCI reductions occur along E-W oriented walkways in the southern part of the study area. The figure also suggests that adding street trees causes the most significant reductions in UTCI over the entire neighborhood. The improvements to thermal comfort are remarkable in some street tree locations, corresponding to the dark blue pixels shown in Figure 7.10(c).

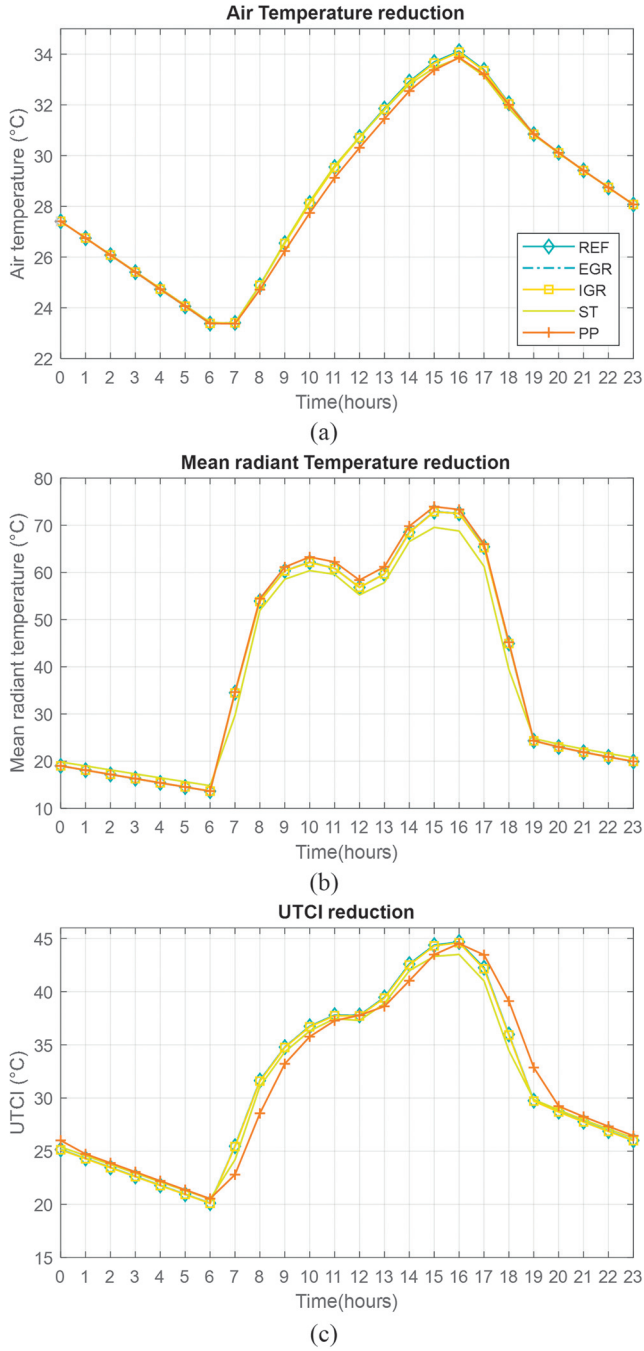

FIGURE 7.9 Diurnal profiles of the performance of NBS in heat mitigation: (a) air temperature reduction; (b) mean radiant temperature reduction; (c) UTCI reduction.

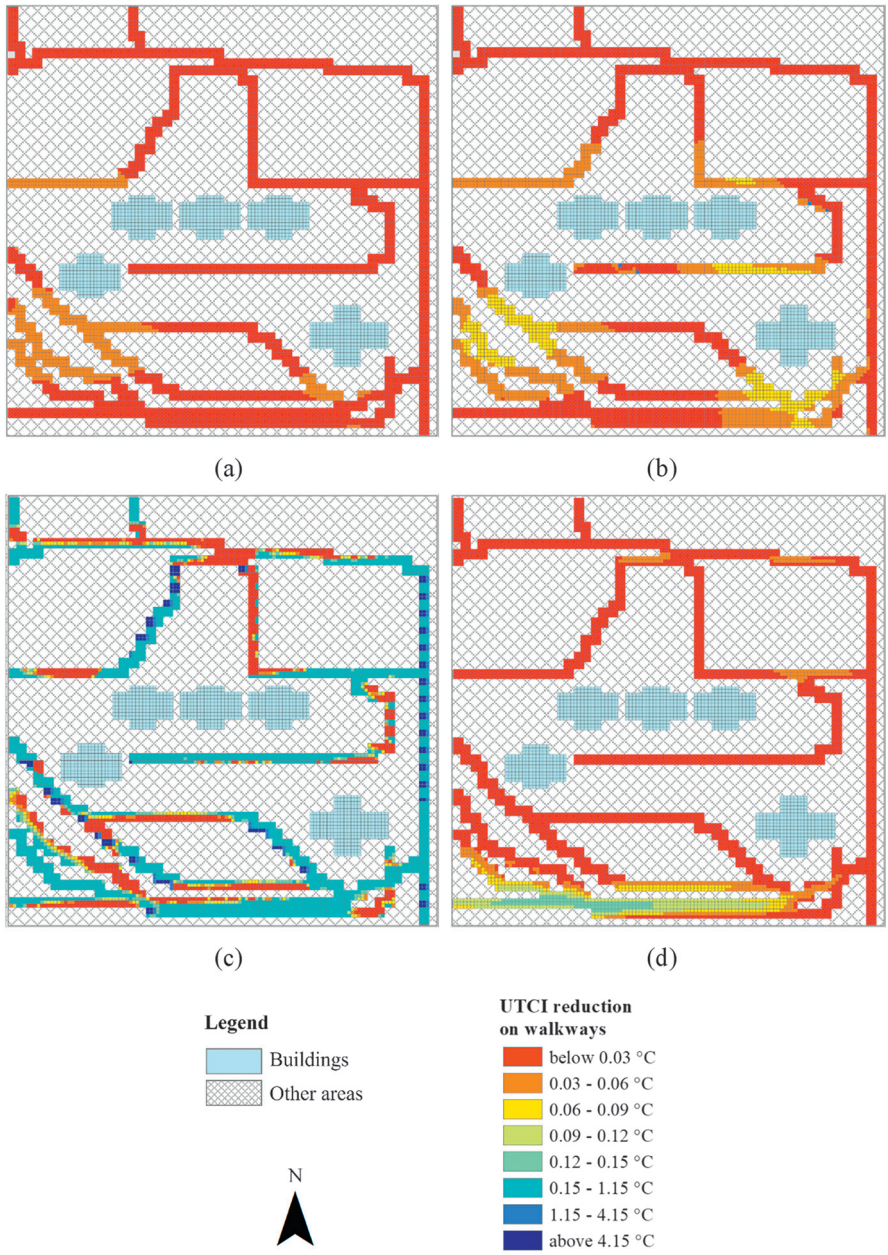

FIGURE 7.10 Distributions of UTCI reductions for all NBS: (a) EGR; (b) IGR; (c) ST; (d) PP.

Performance of Nature-Based Solutions in Building Energy Savings

The proposed integrated modeling framework was used to simulate the energy use of buildings in six cities with varying local climates over a one-year period. We compared the energy consumption of buildings installing green roofs to a reference building using concrete roofs without any energy-saving strategies. The comparison results are shown in Figure 7.11, which displays the annual reduction of both cooling and heating energy by green roofs in each city. Figure 7.11(a) and (b) show the effects of climate and urban built environment (characterized by LCZs) on both cooling and heating building energy savings by green roofs, respectively.

Observed from Figure 7.11(a), the mean reduction of green roofs ranged from 63.38% to 83.21% among the six evaluated cities. The best cooling energy reduction effects for green roofs were observed in London and Sao Paulo, respectively, with mean reduction rates of 78.63% and 83.21% across different built environments. The heating energy reduction effect of green roofs was relatively significant in Sao Paulo, Cairo, and Los Angeles with mean reduction rates of 87.92%, 85.65%, and 80.37%, respectively. Observed from Figure 7.11(b), urban built environment plays a crucial role in determining the green roof energy-saving performance. Significant variations in both cooling and heating energy reductions were observed in different LCZs, with mean reduction rate ranging from 38.38% to 100% for cooling energy reduction and 47.4% to 100% for heating energy reduction. Notably, LCZs 3 and 6, characterized by low-rise buildings, can achieve nearly zero annual energy demands for cooling or heating by installing green roofs. The results indicate that the energy-saving effectiveness of green roofs largely depends on the climate zones they are applied in and the urban built environment.

DISCUSSION

The Effectiveness of NBS in Cooling the Environment and Improving Thermal Comfort

The simulation results show the effectiveness of different NBS towards cooling the environment and improving thermal comfort. Trees and vegetation seem to be the key strategy to reduce temperature and improve thermal comfort in hot summer conditions through their combined effects of shading and evapotranspiration (Ali-Toudert & Mayer, 2007; Makaremi et al., 2012; Wang & Akbari, 2016). At night, the mean radiant temperature of the street tree (ST) scenario is higher than that of the reference. This may be explained by the subdued evapotranspiration of vegetation at nighttime (Peng et al., 2020). Although many existing studies conclude that green roofs have no cooling effect on pedestrian-level microclimate (Chen et al., 2009; Zölch et al., 2016), this study finds that there is some cooling brought about by roof-level heat mitigation strategies, especially by the intensive green roofs (IGR). The more voluminous biomass and extended canopy areas of IGR may provide some passive cooling at the pedestrian-level through evapotranspiration (Peng & Jim, 2013).

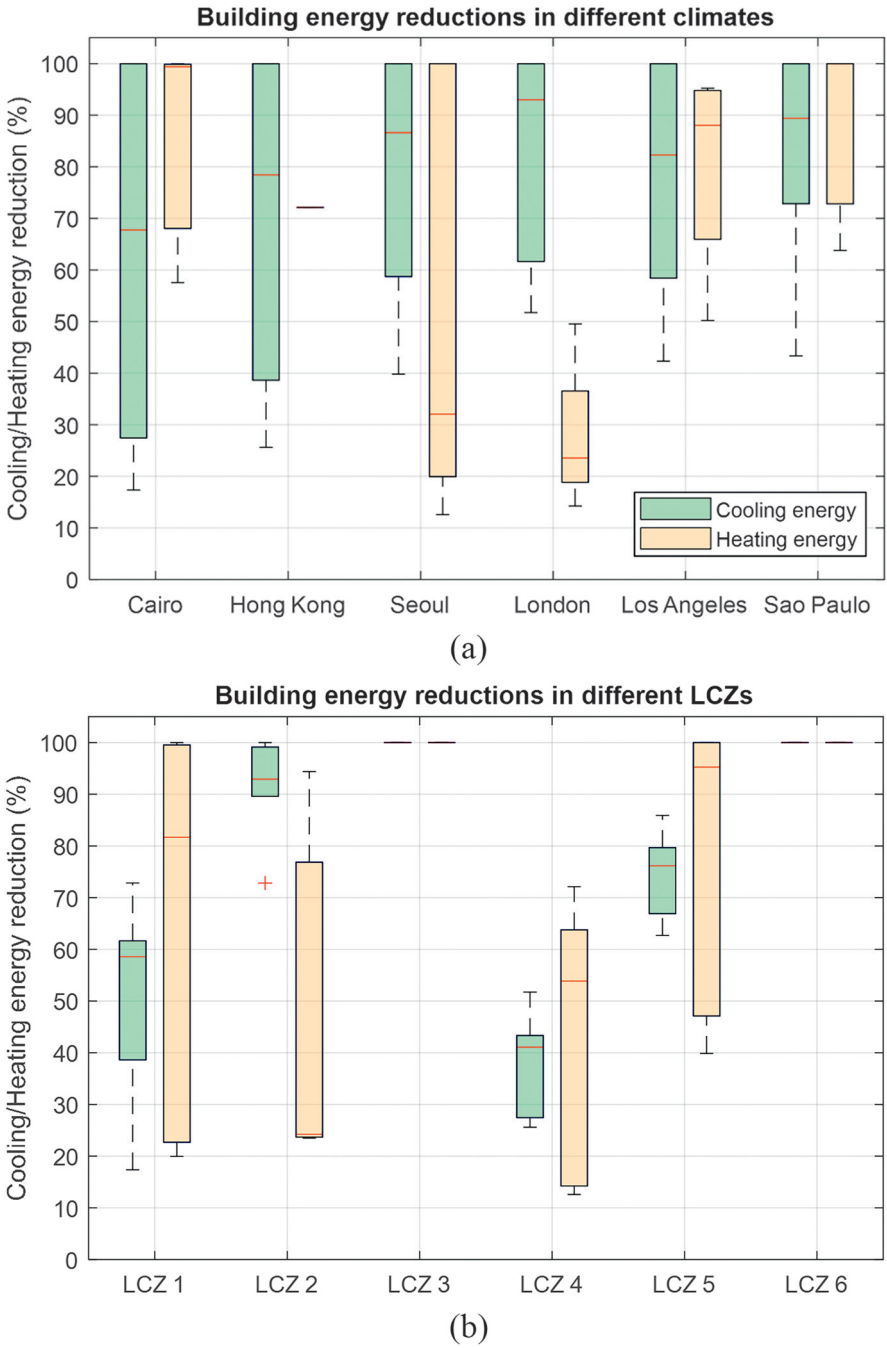

FIGURE 7.11 Annual cooling/heating energy reductions by green roofs: (a) in different climates: (b) in different LCZs.

Among all evaluated types of NBS, street trees cause the biggest reduction in average UTCI, with a maximum reduction of 0.8817 °C at 11:00, while the extensive green roof (EGR) has the least effect on UTCI. For the ST scenario, UTCI reductions are the most significant at the locations where the trees are planted. Other types of heat mitigation strategies also lead to UTCI reductions but to a lesser extent than street trees. These other mitigation strategies also show some locational variation in UTCI reduction. For example, permeable pavement (PP) shows more noticeable effects at the paths located in the south region of the study area, and IGR causes more obvious changes along the E–W directions of buildings. Therefore, location effects may be considered when planning green infrastructure.

Although adding street trees is beneficial, its implementation in well-established, densely populated urban areas may face some challenges. First, there is often less land space than is required to plant a tree and have it develop a mature root system. Second, as a city with a large number of tropical cyclones, falling trees often disrupt traffic and pose a public hazard in Hong Kong. These challenges necessitate the proper choosing of trees and planting strategies. In addition to street trees, some studies also recommend the use of protrusions from façades or buildings located next to the streets to reduce thermal stress exposure and improve walkability (Rodríguez-Algeciras et al., 2017). Such features are not evaluated in this study due to the difficulty of retrofitting existing buildings.

The Effectiveness of Green Roofs in Reducing Building Energy Use

In hot and sunny regions and relatively cold regions, green roofs can reliably reduce energy demand throughout the year. This finding is consistent with existing literature (Costanzo et al., 2016; Silva et al., 2016; Yang et al., 2018; Zinzi & Agnoli, 2012). Due to the extra insulation soil layer of green roofs, which tends to keep heat stored in the buildings, green roofs can provide heating energy-saving benefits as well in cities with colder climates. However, in some warm regions with cloudy or rainy climates, where greenery has less cooling effect due to reduced rates of evaporation and transpiration of plants, the use of green roofs may be carefully considered. Under this case, cool/reflective pavements with higher albedo (e.g., cool roofs) maybe adopted for reducing cooling energy use of buildings. The kinds of strategies reduce surface and air temperature in the surrounding environment mainly by increasing the percentage of reflected solar radiation due to an increase of reflectivity (Mohajerani et al., 2017; Wang et al., 2021). In addition, since urban built environment can significantly affect the performance of green roofs, the possible overshadowing effects of adjacent buildings should be carefully considered and modeled. Some studies also recommend conducting solar simulation before implementing these mitigation strategies (Wong et al., 2021).

When deciding on the implementation of green roofs in the long-term development of buildings, it is also important to consider not only their effectiveness in reducing energy consumption but also their economic and environmental benefits. For example, compared to cool roofs, green roofs provide additional benefits such as reducing urban heat island effects, improving air quality, increasing water-permeable surface, enhancing stormwater management, and improving the

durability of roof materials (Hamel et al., 2021; Meng et al., 2022; Wong et al., 2021). Especially in high-urbanized regions, the application of green roofs can bring more ecosystem service benefits to both urban environments and humans.

CONCLUSION

Given the growing issue of urban heat islands (UHI) and increasing global building energy demand, this study aimed to assess the effectiveness of various nature-based solutions (NBS), including green roofs, permeable pavements, and street trees, in mitigating UHI, improving thermal comfort, and reducing building energy consumption. To improve modeling accuracy, this study developed an integrated modeling approach that combines climate change modeling and building energy simulation to quantify the impact of microclimate change on building energy demand. Through scenario analysis, the impacts of each NBS scenario on air temperature (T_a) reduction, mean radiant temperature (T_{mrt}) reduction, and Universal Thermal Climate Index (UTCI) reduction were analyzed. Our results show that ST scenario was the most effective in reducing T_a, T_{mrt}, and UTCI. However, the effectiveness of each type of NBS varied depending on the location within the study area, highlighting the importance of considering urban forms in infrastructure planning. To further investigate the potential for NBS to reduce building energy consumption, we evaluated the energy-saving performance of green roofs across different ambient climates and urban environments in six global cities: Cairo, Hong Kong, Seoul, London, Los Angeles, and Sao Paulo.

In summary, this study provides important insights into the effects of local ambient climate and urban built environment on the performance of typical NBS in UHI mitigation and building energy savings, which can inform the selection and design of appropriate NBS for different urban contexts to cope with climate change. Limitations of the study however include the fact that this paper largely depends on computer simulations, while the large-scale and long-term experimental data for energy use in buildings are yet to be carried out globally for different NBS. Future works should incorporate this experimental data to gain a better understanding of the holistic potential of NBS under different ambient environments. By incorporating wider study areas, more specific advice can be provided for cooling the urban environment, reducing building energy use and greenhouse gas emissions globally.

REFERENCES

Abdel-Ghany, A. M., Al-Helal, I. M., & Shady, M. R. (2013). Human Thermal Comfort and Heat Stress in an Outdoor Urban Arid Environment: A Case Study. *Advances in Meteorology*, 2013, 1–7. 10.1155/2013/693541

Acero, J. A., & Arrizabalaga, J. (2016). Evaluating the performance of ENVI-met model in diurnal cycles for different meteorological conditions. *Theoretical and Applied Climatology*, 131(1–2), 455–469. 10.1007/s00704-016-1971-y

Ali-Toudert, F., & Mayer, H. (2006). Numerical study on the effects of aspect ratio and orientation of an urban street canyon on outdoor thermal comfort in hot and dry climate. *Building and Environment*, 41(2), 94–108. 10.1016/j.buildenv.2005.01.013

Ali-Toudert, F., & Mayer, H. (2007). Effects of asymmetry, galleries, overhanging façades and vegetation on thermal comfort in urban street canyons. *Solar Energy*, 81(6), 742–754. 10.1016/j.solener.2006.10.007

Aram, F., Higueras Garcia, E., Solgi, E., & Mansournia, S. (2019). Urban green space cooling effect in cities. *Heliyon*, 5(4), e01339. 10.1016/j.heliyon.2019.e01339

ASHRAE, F. (2013). *Fundamentals handbook*. IP Edition, 21.

Barrio, D. (1998). Analysis of the green roofs cooling potential in buildings.

Bedford, T., & Warner, C. (1934). The globe thermometer in studies of heating and ventilation. *Epidemiology & Infection*, 34(4), 458–473.

Berardi, U. (2016). The outdoor microclimate benefits and energy saving resulting from green roofs retrofits. *Energy and Buildings*, 121, 217–229. 10.1016/j.enbuild.2016.03.021

Bianchini, F., & Hewage, K. (2012). How "green" are the green roofs? Lifecycle analysis of green roof materials. *Building and Environment*, 48, 57–65. 10.1016/j.buildenv.2011.08.019

Bruse, M., & Fleer, H. (1998). Simulating surface–plant–air interactions inside urban environments with a three dimensional numerical model. *Environmental Modelling & Software*, 13(3-4), 373–384.

Castleton, H. F., Stovin, V., Beck, S. B. M., & Davison, J. B. (2010). Green roofs; building energy savings and the potential for retrofit. *Energy and Buildings*, 42(10), 1582–1591. 10.1016/j.enbuild.2010.05.004

Chen, H., Ooka, R., Huang, H., & Tsuchiya, T. (2009). Study on mitigation measures for outdoor thermal environment on present urban blocks in Tokyo using coupled simulation. *Building and Environment*, 44(11), 2290–2299. 10.1016/j.buildenv.2009.03.012

Chen, Y.-C., Lin, T.-P., & Matzarakis, A. (2014). Comparison of mean radiant temperature from field experiment and modelling: a case study in Freiburg, Germany. *Theoretical and Applied Climatology*, 118(3), 535–551. 10.1007/s00704-013-1081-z

Cheng, V., Ng, E., Chan, C., & Givoni, B. (2011). Outdoor thermal comfort study in a sub-tropical climate: a longitudinal study based in Hong Kong. *International Journal of Biometeorology*, 56(1), 43–56. 10.1007/s00484-010-0396-z

Cheung, P. K., & Jim, C. Y. (2018a). Comparing the cooling effects of a tree and a concrete shelter using PET and UTCI. *Building and Environment*, 130, 49–61. 10.1016/j.buildenv.2017.12.013

Cheung, P. K., & Jim, C. Y. (2018b). Subjective outdoor thermal comfort and urban green space usage in humid-subtropical Hong Kong. *Energy and Buildings*, 173, 150–162. 10.1016/j.enbuild.2018.05.029

Comfort, A. S. o. C. E. T. C. o. O. H. (2003). Outdoor Human Comfort and Its Assessment: State of the Art.

Costanzo, V., Evola, G., & Marletta, L. (2016). Energy savings in buildings or UHI mitigation? Comparison between green roofs and cool roofs. *Energy and Buildings*, 114, 247–255. 10.1016/j.enbuild.2015.04.053

Crank, P. J., Middel, A., Wagner, M., Hoots, D., Smith, M., & Brazel, A. (2020). Validation of seasonal mean radiant temperature simulations in hot arid urban climates. *Science of The Total Environment*, 749. 10.1016/j.scitotenv.2020.141392

Crawley, D. B., Lawrie, L. K., Winkelmann, F. C., Buhl, W. F., Huang, Y. J., Pedersen, C. O., Strand, R. K., Liesen, R. J., Fisher, D. E., & Witte, M. J. (2001). EnergyPlus: creating a new-generation building energy simulation program. *Energy and Buildings*, 33(4), 319–331.

Das, M., & Das, A. (2020). Assessing the relationship between local climatic zones (LCZs) and land surface temperature (LST)–A case study of Sriniketan-Santiniketan Planning Area (SSPA), West Bengal, India. *Urban Climate*, 32, 100591.

de Lieto Vollaro, R., Vallati, A., & Bottillo, S. (2013). Differents Methods to Estimate the Mean Radiant Temperature in an Urban Canyon. *Advanced Materials Research*, 650, 647–651. 10.4028/www.scientific.net/AMR.650.647

Doick, K. J., Peace, A., & Hutchings, T. R. (2014). The role of one large greenspace in mitigating London's nocturnal urban heat island. *Science of The Total Environment*, 493, 662–671. 10.1016/j.scitotenv.2014.06.048

Fang, Z., Feng, X., Liu, J., Lin, Z., Mak, C. M., Niu, J., Tse, K.-T., & Xu, X. (2019). Investigation into the differences among several outdoor thermal comfort indices against field survey in subtropics. *Sustainable Cities and Society*, 44, 676–690. 10.101 6/j.scs.2018.10.022

Feyisa, G. L., Dons, K., & Meilby, H. (2014). Efficiency of parks in mitigating urban heat island effect: An example from Addis Ababa. *Landscape and Urban Planning*, 123, 87–95. 10.1016/j.landurbplan.2013.12.008

Fiala, D., Lomas, K. J., & Stohrer, M. (1999). A computer model of human thermoregulation for a wide range of environmental conditions: the passive system. *Journal of Applied Physiology*, 87(5), 1957–1972.

Fiala, D., Lomas, K. J., & Stohrer, M. (2001). Computer prediction of human thermoregulatory and temperature responses to a wide range of environmental conditions. *International Journal of Biometeorology*, 45(3), 143–159.

Fumo, N. (2014). A review on the basics of building energy estimation. *Renewable and Sustainable Energy Reviews*, 31, 53–60. 10.1016/j.rser.2013.11.040

Fumo, N., Mago, P., & Luck, R. (2010). Methodology to estimate building energy consumption using EnergyPlus Benchmark Models. *Energy and Buildings*, 42(12), 2331–2337. 10.1016/j.enbuild.2010.07.027

Gill, S. E., Handley, J. F., Ennos, A. R., & Pauleit, S. (2007). Adapting cities for climate change: the role of the green infrastructure. *Built Environment*, 33(1), 115–133.

Halder, B., Bandyopadhyay, J., & Banik, P. (2021). Monitoring the effect of urban development on urban heat island based on remote sensing and geo-spatial approach in Kolkata and adjacent areas, India. *Sustainable Cities and Society*, 74. 10.1016/ j.scs.2021.103186

Hamel, P., Guerry, A. D., Polasky, S., Han, B., Douglass, J. A., Hamann, M., Janke, B., Kuiper, J. J., Levrel, H., Liu, H., Lonsdorf, E., McDonald, R. I., Nootenboom, C., Ouyang, Z., Remme, R. P., Sharp, R. P., Tardieu, L., Viguié, V., Xu, D., Zheng, H., & Daily, G. C. (2021). Mapping the benefits of nature in cities with the InVEST software. *npj Urban Sustainability*, 1(1). 10.1038/s42949-021-00027-9

Haselbach, L. (2009). Pervious concrete and mitigation of the urban heat island effect.

He, Y., Yu, H., Ozaki, A., & Dong, N. (2020). Thermal and energy performance of green roof and cool roof: A comparison study in Shanghai area. *Journal of Cleaner Production*, 267. 10.1016/j.jclepro.2020.122205

He, Y., Yu, H., Ozaki, A., Dong, N., & Zheng, S. (2017). Influence of plant and soil layer on energy balance and thermal performance of green roof system. *Energy*, 141, 1285–1299. 10.1016/j.energy.2017.08.064

Herath, H. M. P. I. K., Halwatura, R. U., & Jayasinghe, G. Y. (2018). Evaluation of green infrastructure effects on tropical Sri Lankan urban context as an urban heat island adaptation strategy. *Urban Forestry & Urban Greening*, 29, 212–222. 10.1016/j.ufug. 2017.11.013

Herrmann, J., & Matzarakis, A. (2010). Influence of mean radiant temperature on thermal comfort of humans in idealized urban environments. *Berichte des Meteorologischen Instituts der Albert-Ludwigs-Universität Freiburg*, 522.

Hien, W. N., Ignatius, M., Eliza, A., Jusuf, S. K., & Samsudin, R. (2012). Comparison of STEVE and ENVI-met as temperature prediction models for Singapore context.

International Journal of Sustainable Building Technology and Urban Development, 3(3), 197–209. 10.1080/2093761x.2012.720224

Höppe, P. (1992). A new procedure to determine the mean radiant temperature outdoors. *Wetter und Leben*, 44, 147–151.

Höppe, P. (1999). The physiological equivalent temperature–a universal index for the biometeorological assessment of the thermal environment. *International Journal of Biometeorology*, 43(2), 71–75.

Hosseini, M., Bigtashi, A., & Lee, B. (2020). A systematic approach in constructing typical meteorological year weather files using machine learning. *Energy and Buildings*, 226. 10.1016/j.enbuild.2020.110375

Huttner, S. (2012). *Further development and application of the 3D microclimate simulation ENVI-met*. Mainz: Johannes Gutenberg-Universitat in Mainz, 147.

ITO, M. (2006). Study on pavement technologies to mitigate the heat island effect and their effectiveness.

Jia, S., & Wang, Y. (2021). Effect of heat mitigation strategies on thermal environment, thermal comfort, and walkability: A case study in Hong Kong. *Building and Environment*, 201. 10.1016/j.buildenv.2021.107988

Kabisch, N., Korn, H., Stadler, J., & Bonn, A. (2017). *Nature-based solutions to climate change adaptation in urban areas: Linkages between science, policy and practice*. Springer Nature.

Ketterer, C., & Matzarakis, A. (2015). Comparison of different methods for the assessment of the urban heat island in Stuttgart, Germany. *International Journal of Biometeorology*, 59(9), 1299–1309. 10.1007/s00484-014-0940-3

Kim, S. W., & Brown, R. D. (2021). Urban heat island (UHI) variations within a city boundary: A systematic literature review. *Renewable and Sustainable Energy Reviews*, 148. 10.1016/j.rser.2021.111256

Kuehn, L., Stubbs, R., & Weaver, R. (1970). Theory of the globe thermometer. *Journal of Applied Physiology*, 29(5), 750–757.

Lafortezza, R., Chen, J., van den Bosch, C. K., & Randrup, T. B. (2018). Nature-based solutions for resilient landscapes and cities. *Environmental Research*, 165, 431–441. 10.1016/j.envres.2017.11.038

Lai, D., Guo, D., Hou, Y., Lin, C., & Chen, Q. (2014). Studies of outdoor thermal comfort in northern China. *Building and Environment*, 77, 110–118. 10.1016/j.buildenv.2014.03.026

Li, X., Zhou, Y., Yu, S., Jia, G., Li, H., & Li, W. (2019). Urban heat island impacts on building energy consumption: A review of approaches and findings. *Energy*, 174, 407–419. 10.1016/j.energy.2019.02.183

Luo, N., Wang, Z., Blum, D., Weyandt, C., Bourassa, N., Piette, M. A., & Hong, T. (2022). A three-year dataset supporting research on building energy management and occupancy analytics. *Scientific Data*, 9(1), 156. 10.1038/s41597-022-01257-x

Makaremi, N., Salleh, E., Jaafar, M. Z., & GhaffarianHoseini, A. (2012). Thermal comfort conditions of shaded outdoor spaces in hot and humid climate of Malaysia. *Building and Environment*, 48, 7–14. 10.1016/j.buildenv.2011.07.024

Manavvi, S., & Rajasekar, E. (2020). Estimating outdoor mean radiant temperature in a humid subtropical climate. *Building and Environment*, 171. 10.1016/j.buildenv.2020.106658

Mayer, H., & Höppe, P. (1987). Thermal comfort of man in different urban environments. *Theoretical and Applied Climatology*, 38(1), 43–49.

Mehrotra, S., Bardhan, R., & Ramamritham, K. (2019). Outdoor thermal performance of heterogeneous urban environment: An indicator-based approach for climate-sensitive planning. *Science of The Total Environment*, 669, 872–886. 10.1016/j.scitotenv.2019.03.152

Meng, L., Zhou, Y., Roman, M. O., Stokes, E. C., Wang, Z., Asrar, G. R., Mao, J., Richardson, A. D., Gu, L., & Wang, Y. (2022). Artificial light at night: an underappreciated effect on phenology of deciduous woody plants. *PNAS Nexus*, 1(2), pgac046. 10.1093/pnasnexus/pgac046

Mohajerani, A., Bakaric, J., & Jeffrey-Bailey, T. (2017). The urban heat island effect, its causes, and mitigation, with reference to the thermal properties of asphalt concrete. *Journal of Environmental Management*, 197, 522–538. 10.1016/j.jenvman.2017.03.095

Morakinyo, T. E., Dahanayake, K. W. D. K. C., Ng, E., & Chow, C. L. (2017). Temperature and cooling demand reduction by green-roof types in different climates and urban densities: A co-simulation parametric study. *Energy and Buildings*, 145, 226–237. 10.1016/j.enbuild.2017.03.066

Morakinyo, T. E., Kong, L., Lau, K. K.-L., Yuan, C., & Ng, E. (2017). A study on the impact of shadow-cast and tree species on in-canyon and neighborhood's thermal comfort. *Building and Environment*, 115, 1–17. 10.1016/j.buildenv.2017.01.005

Nikolopoulou, M., Baker, N., & Steemers, K. (2001). Thermal comfort in outdoor urban spaces: understanding the human parameter. *Solar Energy*, 70(3), 227–235.

Niachou, A., Papakonstantinou, K., Santamouris, M., Tsangrassoulis, A., Mihalakakou, G. (2001). Analysis of the green roof thermal properties and investigation of its energy performance. *Energy and Buildings*, 33, 719–729.

Patel, P., Kalyanam, R., He, L., Aliaga, D., & Niyogi, D. (2023). Deep learning-based urban morphology for city-scale environmental modeling. *PNAS Nexus*, 2(3), pgad027. 10.1093/pnasnexus/pgad027

Peng, L., & Jim, C. (2013). Green-Roof Effects on Neighborhood Microclimate and Human Thermal Sensation. *Energies*, 6(2), 598–618. 10.3390/en6020598

Peng, L. L. H., Jiang, Z., Yang, X., He, Y., Xu, T., & Chen, S. S. (2020). Cooling effects of block-scale facade greening and their relationship with urban form. *Building and Environment*, 169. 10.1016/j.buildenv.2019.106552

Profiroiu, C. M., Bodislav, D. A., Burlacu, S., & Rădulescu, C. V. (2020). Challenges of sustainable urban development in the context of population Growth. *European Journal of Sustainable Development*, 9(3), 51- 51.

Provencal, S., Bergeron, O., Leduc, R., & Barrette, N. (2016). Thermal comfort in Quebec City, Canada: sensitivity analysis of the UTCI and other popular thermal comfort indices in a mid-latitude continental city. *International Journal of Biometeorology*, 60(4), 591–603. 10.1007/s00484-015-1054-2

Rakha, T. (2015). Towards comfortable and walkable cities: spatially resolved outdoor thermal comfort analysis linked to travel survey-based human activity schedules. Massachusetts Institute of Technology.

Razzaghmanesh, M., Beecham, S., & Salemi, T. (2016). The role of green roofs in mitigating Urban Heat Island effects in the metropolitan area of Adelaide, South Australia. *Urban Forestry & Urban Greening*, 15, 89–102. 10.1016/j.ufug.2015.11.013

Ritchie, H., & Roser, M. (2018). Urbanization. Our world in data.

Rodríguez-Algeciras, J., Tablada, A., & Matzarakis, A. (2017). Effect of asymmetrical street canyons on pedestrian thermal comfort in warm-humid climate of Cuba. *Theoretical and Applied Climatology*, 133(3-4), 663–679. 10.1007/s00704-017-2204-8

Romeo, C., & Zinzi, M. (2013). Impact of a cool roof application on the energy and comfort performance in an existing non-residential building. A Sicilian case study. *Energy and Buildings*, 67, 647–657. 10.1016/j.enbuild.2011.07.023

Sailor, D. J. (2008). A green roof model for building energy simulation programs. *Energy and Buildings*, 40(8), 1466–1478. 10.1016/j.enbuild.2008.02.001

Santamouris, M. (2013). Using cool pavements as a mitigation strategy to fight urban heat island—A review of the actual developments. *Renewable and Sustainable Energy Reviews*, 26, 224–240. 10.1016/j.rser.2013.05.047

Schwaab, J., Meier, R., Mussetti, G., Seneviratne, S., Burgi, C., & Davin, E. L. (2021). The role of urban trees in reducing land surface temperatures in European cities. *Nature Communication*, 12(1), 6763. 10.1038/s41467-021-26768-w

Silva, C. M., Gomes, M. G., & Silva, M. (2016). Green roofs energy performance in Mediterranean climate. *Energy and Buildings*, 116, 318–325. 10.1016/j.enbuild.2016.01.012

Spagnolo, J., & de Dear, R. (2003). A field study of thermal comfort in outdoor and semi-outdoor environments in subtropical Sydney Australia. *Building and Environment*, 38(5), 721–738. 10.1016/s0360-1323(02)00209-3

Standard, I., & ISO, B. (1998). Ergonomics of the thermal environment—instruments for measuring physical quantities.

Stewart, I. D., & Oke, T. R. (2012). Local climate zones for urban temperature studies. *Bulletin of the American Meteorological Society*, 93(12), 1879–1900.

Su, W., Zhang, L., & Chang, Q. (2022). Nature-based solutions for urban heat mitigation in historical and cultural block: The case of Beijing Old City. *Building and Environment*, 225. 10.1016/j.buildenv.2022.109600

Susca, T., Gaffin, S. R., & Dell'osso, G. R. (2011). Positive effects of vegetation: urban heat island and green roofs. *Environmental Pollution*, 159(8-9), 2119–2126. 10.1016/j.envpol.2011.03.007

Takebayashi, H., & Moriyama, M. (2012). Study on Surface Heat Budget of Various Pavements for Urban Heat Island Mitigation. *Advances in Materials Science and Engineering*, 2012, 1–11. 10.1155/2012/523051

Taleghani, M. (2018). Outdoor thermal comfort by different heat mitigation strategies- A review. *Renewable and Sustainable Energy Reviews*, 81, 2011–2018. 10.1016/j.rser.2017.06.010

Tan, C. L., Wong, N. H., & Jusuf, S. K. (2013). Outdoor mean radiant temperature estimation in the tropical urban environment. *Building and Environment*, 64, 118–129. 10.1016/j.buildenv.2013.03.012

Tan, Z., Lau, K. K.-L., & Ng, E. (2016). Urban tree design approaches for mitigating daytime urban heat island effects in a high-density urban environment. *Energy and Buildings*, 114, 265–274. 10.1016/j.enbuild.2015.06.031

Theodosiou, T. G. (2003). Summer period analysis of the performance of a planted roof as a passive cooling technique. *Energy and Buildings*, 35(9), 909–917. 10.1016/s0378-7788(03)00023-9

Thom, J. K., Coutts, A. M., Broadbent, A. M., & Tapper, N. J. (2016). The influence of increasing tree cover on mean radiant temperature across a mixed development suburb in Adelaide, Australia. *Urban Forestry & Urban Greening*, 20, 233–242. 10.1016/j.ufug.2016.08.016

Thorsson, S., Honjo, T., Lindberg, F., Eliasson, I., & Lim, E.-M. (2007). Thermal comfort and outdoor activity in Japanese urban public places. *Environment and Behavior*, 39(5), 660–684.

Thorsson, S., Lindberg, F., Eliasson, I., & Holmer, B. (2007). Different methods for estimating the mean radiant temperature in an outdoor urban setting. *International Journal of Climatology*, 27(14), 1983–1993. 10.1002/joc.1537

Townshend, D. (2007). Study on green roof application in Hong Kong. *Architectural services department*.

VDI. (1998). *Methods for the human-biometerological assessment of climate and air Hygiene for Urban and Regional Planning*. In: Beuth Berlin.

Walikewitz, N., Jänicke, B., Langner, M., Meier, F., & Endlicher, W. (2015). The difference between the mean radiant temperature and the air temperature within indoor environments: A case study during summer conditions. *Building and Environment*, 84, 151–161. 10.1016/j.buildenv.2014.11.004

Wang, C., Wang, Z.-H., Kaloush, K. E., & Shacat, J. (2021). Cool pavements for urban heat island mitigation: A synthetic review. *Renewable and Sustainable Energy Reviews*, 146. 10.1016/j.rser.2021.111171

Wang, Y., & Akbari, H. (2016). Analysis of urban heat island phenomenon and mitigation solutions evaluation for Montreal. *Sustainable Cities and Society*, 26, 438–446. 10.1016/j.scs.2016.04.015

Wong, N. H., Jusuf, S. K., Syafii, N. I., Chen, Y., Hajadi, N., Sathyanarayanan, H., & Manickavasagam, Y. V. (2011). Evaluation of the impact of the surrounding urban morphology on building energy consumption. *Solar Energy*, 85(1), 57–71. 10.1016/j.solener.2010.11.002

Wong, N. H., Tan, C. L., Kolokotsa, D. D., & Takebayashi, H. (2021). Greenery as a mitigation and adaptation strategy to urban heat. *Nature Reviews Earth & Environment*, 2(3), 166–181. 10.1038/s43017-020-00129-5

Xi, T., Li, Q., Mochida, A., & Meng, Q. (2012). Study on the outdoor thermal environment and thermal comfort around campus clusters in subtropical urban areas. *Building and Environment*, 52, 162–170.

Yamada, T., & Mellor, G. (1975). A simulation of the Wangara atmospheric boundary layer data. *Journal of Atmospheric Sciences*, 32(12), 2309–2329.

Yamamoto, Y. (2006). Measures to mitigate urban heat islands (1349-3663).

Yang, J., Mohan Kumar, D. l., Pyrgou, A., Chong, A., Santamouris, M., Kolokotsa, D., & Lee, S. E. (2018). Green and cool roofs' urban heat island mitigation potential in tropical climate. *Solar Energy*, 173, 597–609. 10.1016/j.solener.2018.08.006

Yang, J., Ren, J., Sun, D., Xiao, X., Xia, J. C., Jin, C., & Li, X. (2021). Understanding land surface temperature impact factors based on local climate zones. *Sustainable Cities and Society*, 69, 102818.

Yang, J., Xin, J., Zhang, Y., Xiao, X., & Xia, J. C. (2022). Contributions of sea–land breeze and local climate zones to daytime and nighttime heat island intensity. *NPJ Urban Sustainability*, 2(1), 12.

Yang, Y., Gatto, E., Gao, Z., Buccolieri, R., Morakinyo, T. E., & Lan, H. (2019). The "plant evaluation model" for the assessment of the impact of vegetation on outdoor microclimate in the urban environment. *Building and Environment*, 159. 10.1016/j.buildenv.2019.05.029

Yu, C., & Hien, W. N. (2006). Thermal benefits of city parks. *Energy and Buildings*, 38(2), 105–120. 10.1016/j.enbuild.2005.04.003

Zhao, M., Srebric, J., Berghage, R. D., & Dressler, K. A. (2015). Accumulated snow layer influence on the heat transfer process through green roof assemblies. *Building and Environment*, 87, 82–91. 10.1016/j.buildenv.2014.12.018

Zheng, Y., Ren, C., Xu, Y., Wang, R., Ho, J., Lau, K., & Ng, E. (2018). GIS-based mapping of Local Climate Zone in the high-density city of Hong Kong. *Urban Climate*, 24, 419–448. 10.1016/j.uclim.2017.05.008

Zheng, Y., & Weng, Q. (2020). Modeling the Effect of Green Roof Systems and Photovoltaic Panels for Building Energy Savings to Mitigate Climate Change. *Remote Sensing*, 12(15). 10.3390/rs12152402

Zhou, W., Wang, J., & Cadenasso, M. L. (2017). Effects of the spatial configuration of trees on urban heat mitigation: A comparative study. *Remote Sensing of Environment*, 195, 1–12. 10.1016/j.rse.2017.03.043

Zinzi, M., & Agnoli, S. (2012). Cool and green roofs. An energy and comfort comparison between passive cooling and mitigation urban heat island techniques for residential buildings in the Mediterranean region. *Energy and Buildings*, 55, 66–76. 10.1016/j.enbuild.2011.09.024

Zölch, T., Maderspacher, J., Wamsler, C., & Pauleit, S. (2016). Using green infrastructure for urban climate-proofing: An evaluation of heat mitigation measures at the micro-scale. *Urban Forestry & Urban Greening*, 20, 305–316. 10.1016/j.ufug.2016.09.011